

# A Novel Technique for 4-Dimensional Atmosphere and Oceanographic Irradiance Measurements Using 3-D Spatial Filtering

AD-A283 758



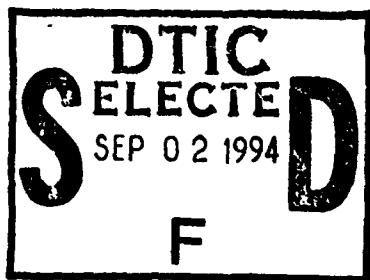
①

Contract No. N00014-94-C-0099

Period of Performance: 04/14/94 to 09/30/94

## Bi-Monthly Report

Reporting Period: 06/01/94 to 07/31/94



*Presented to:*

Office of Naval Research  
Ballston Tower One  
800 North Quincy Street  
Arlington, VA 22217-5660

*Scientific Officer:*

Steve Ackleson

This document has been approved  
for public release and sale; its  
distribution is unlimited.

*Presented by:*

Physical Optics Corporation  
Research and Development Division  
20600 Gramercy Place, Suite 103  
Torrance, California 90501

*Principal Investigator:*

Shudong Wu  
(310) 320-3088

94 8 22 1 7 5

94-26762



798

July 1994

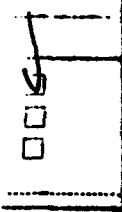
## INTRODUCTION

During the first two months of this project, Physical Optics Corporation (POC) analytically evaluated the depth discrimination properties of a pixel filter. Numerical simulation results indicate that pixel filters have fine depth discrimination capability. Following the numerical analysis, we started to design experiments to verify the capability of the pixel filter. We performed two experiments: first we measured the light intensity as a function of depth; second, we conducted measurements in the frequency domain as a function of depth. In the frequency domain, measurements are insensitive to fluctuations in light intensity; thus, a higher signal/noise ratio can be expected.

### 1.0 DEPTH DISCRIMINATION BASED ON LIGHT INTENSITY

The experimental setup is shown schematically in Figure 1. An argon laser beam is sent through an aperture which filters out scattered stray light. The beam is then turned 90 degrees by a turning mirror. A beamsplitter splits the beam into two subbeams. The first subbeam is turned 90 degrees by a glass reflector on which a visible spot is formed. The spot is imaged by the combination of the imaging lens and CCD. The second subbeam is turned 90 degrees by a mirror and further split into two beams. One of them continues traveling to the left, and is turned 90 degrees by another glass reflector on which a visible spot is formed. This spot is also imaged by the imaging lens and CCD combination. After the second beam splitter, the second beam is expanded with a beam expander and is projected onto a dispersion screen, which forms a background of stray light for the two visible spots on the two glass reflectors. The computer controls the CCD camera which measures the optical intensity of all of the pixels. The intensity of one pre-determined pixel on the CCD camera is recorded, while the intensities of all the other pixels are disregarded. The CCD camera has 16 bit gray level.

During the experiment, the imaging lens/CCD camera was moved axially (as shown in Figure 1) so that the object focal plane of the lens scans across the two visible spots formed by the two subbeams beams on the glass reflectors. These two spots are both on the optical axis. Figure 2 shows the intensity of the pixel as a function of the axial position of the imaging system. The two spots are clearly visible even though they are on the same axis and there is strong background illumination.



Distribution /	
Availability Codes	
Dist	Avail and/or Special
A-1	

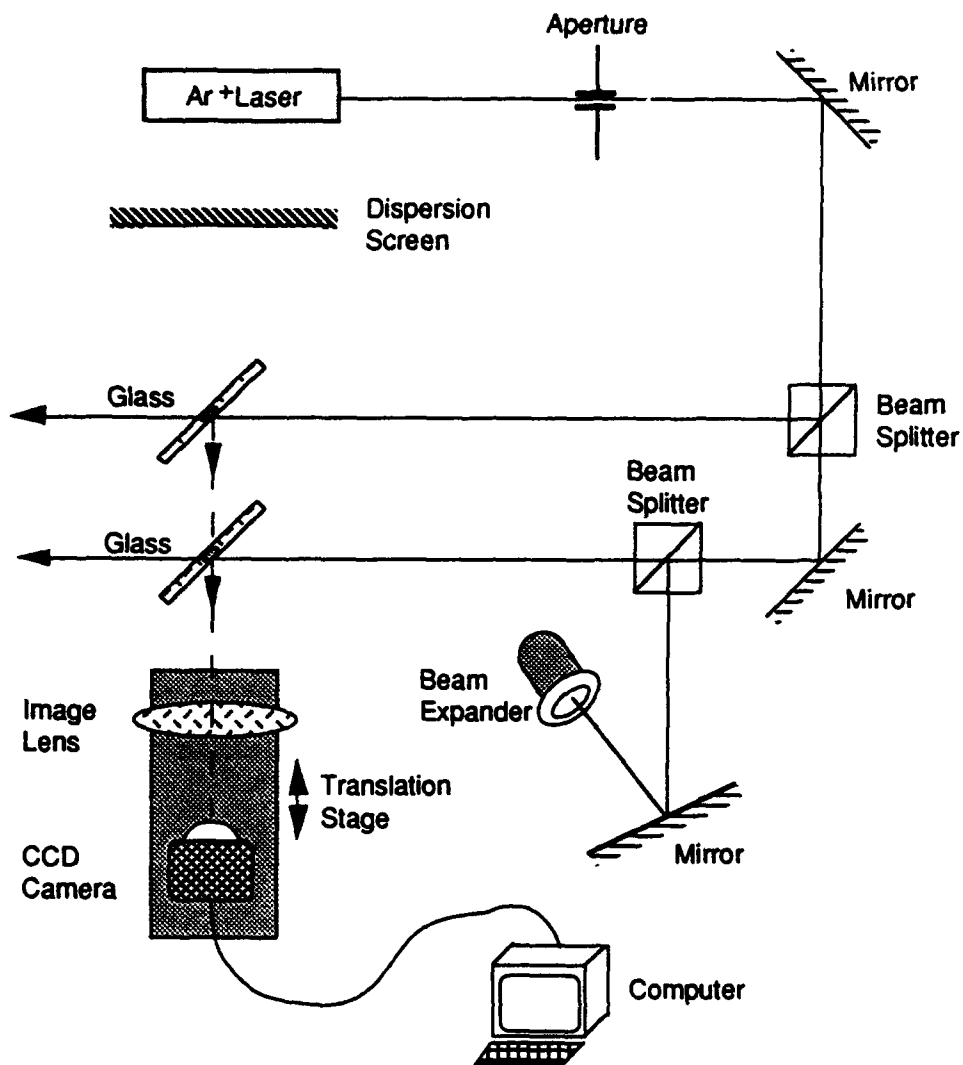


Figure 1  
Setup for measuring depth discrimination based on the intensity of a single pixel of the CCD camera.

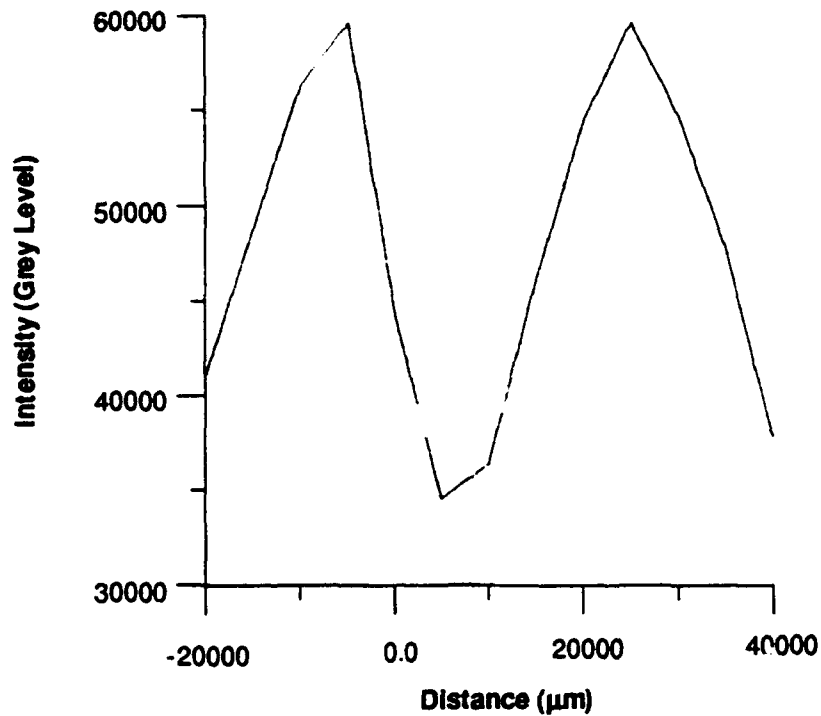


Figure 2  
Intensity level versus axial position (with arbitrary zero point)  
of the objective lens and CCD camera.

## 2.0 DEPTH DISCRIMINATION MEASURED IN THE FREQUENCY DOMAIN

The depth response of a pixel filter imaging system is depicted in Figure 3(a). We have made an observation which allows us to transform the measurement from the intensity to the frequency domain: when the system is in focus, in the neighborhood of  $z = 0$ , the shape of the curve in Figure 3 is approximately that of a second order polynomial. At increased defocus distances, there is a region in which the curve is approximately linear, as shown in Figure 3(a). If we modulate the defocus distance with a sine wave ( $z = a \sin \omega t$ ), let us analyze the response at the detector. First, we consider the frequency component at  $2\omega$ . When the system is in focus,  $I(z) = Az^2 + B$ . Suppose  $z = a \sin \omega t$  and the modulation amplitude  $a$  is small so that the parabolic condition is still valid. Then it follows that

$$\begin{aligned} I(z) &= Az^2 + B \\ &= A(a \sin \omega t)^2 + B \\ &= A[-1/2a(\cos(\omega t + \omega t) - 1)] + B \\ &= -1/2 A \cdot a \cdot \cos(2 \omega t) + 1/2 A \cdot a + B. \end{aligned}$$

This means that when the system is in focus, the detector output consists of a dc component and a component at twice the modulation frequency.

Next, let us consider the linear region in Figure 3(a), where  $I(z) = C \cdot z + D = C \cdot a \cdot \sin \omega t + D$ . The frequency component at  $2\omega$  is zero; at  $\omega$  it is not zero.

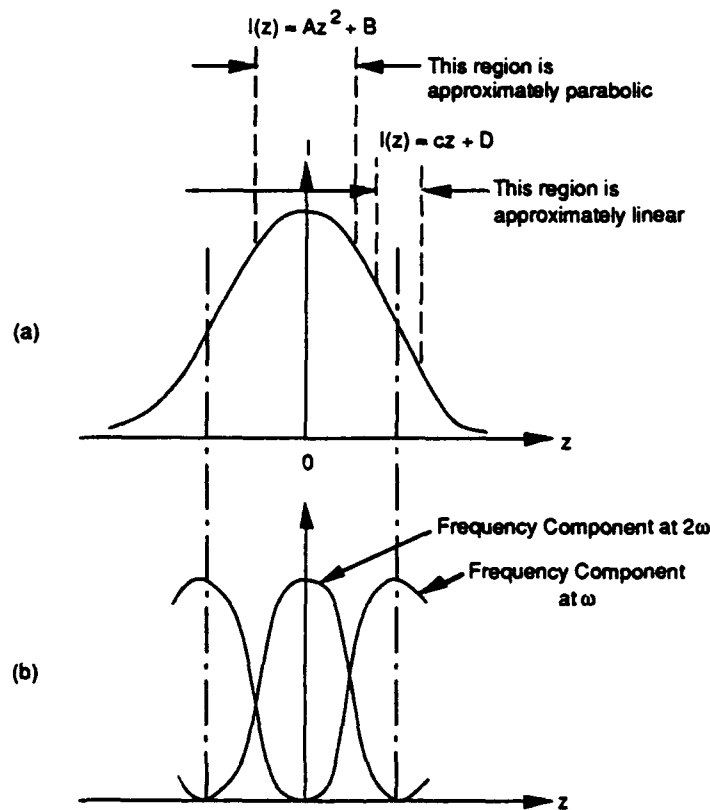


Figure 3  
(a) Intensity as a function of defocus distance  $z$ . (b) Frequency components at  $\omega$  and  $2\omega$ .

The frequency components at  $\omega$  and  $2\omega$  are depicted in Figure 3(b). Comparing Figure 3(b) with Figure 3(a), we notice that at the defocus position  $z$  where the second harmonic becomes zero, the intensity curve in Figure 3(a) is still far above zero. This indicates that the  $2\omega$  curve is sharper than the intensity curve, and thus that its resolution on the  $z$  axis can be higher than that of the intensity curve.

The experimental setup for the measurement of the frequency components is shown in Figure 4. The modulation is generated by a loudspeaker, whose vibrating membrane produces a small sinusoidal displacement. A photodetector with a lens is attached to the membrane. The detector has a small active area, eliminating the need for a pinhole. A lock-in amplifier is used to amplify the frequency component while suppressing other components.

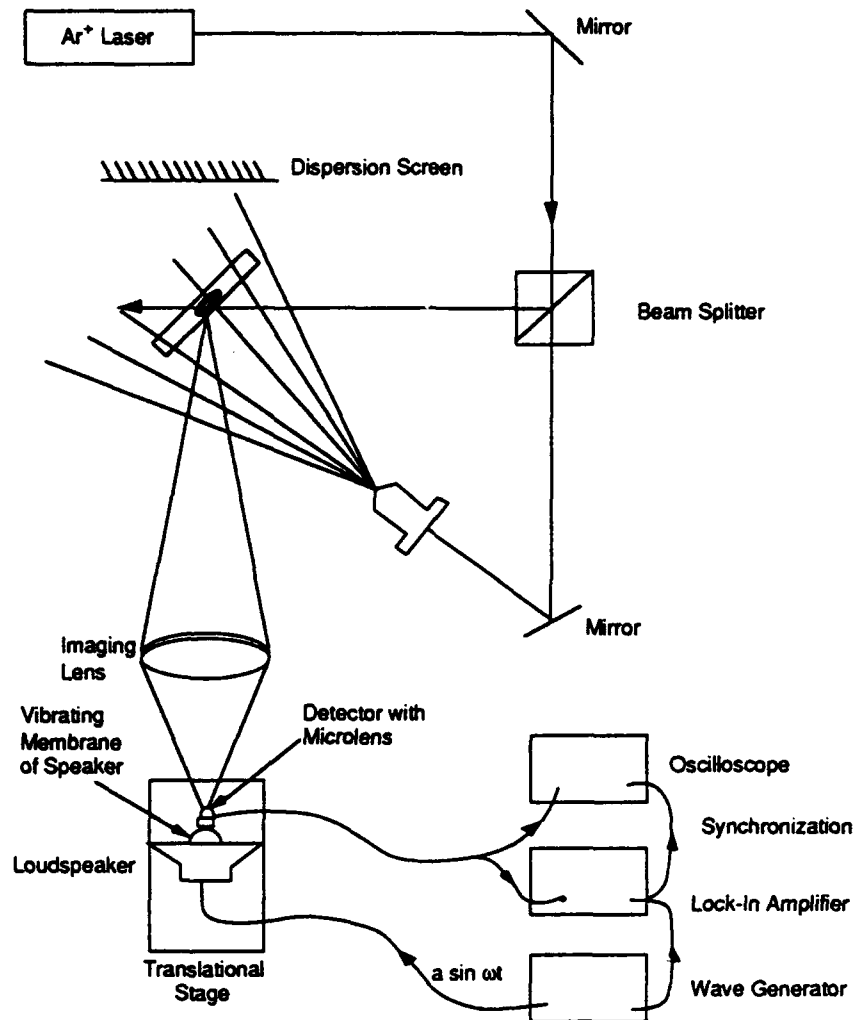


Figure 4  
Experimental setup to take measurements in the frequency domain.

Preliminary results confirm that the second harmonic indeed peaks at the in-focus position and decreases significantly outside of that position. Figure 5 shows the measured second harmonic.

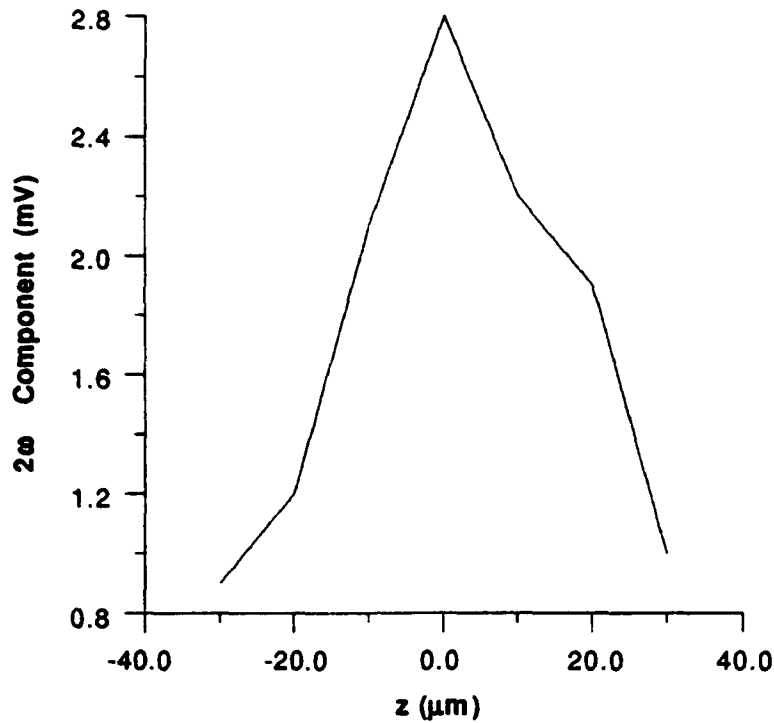


Figure 5  
Amplitude of  $2\omega$  frequency components versus axial position.

We are fine tuning the experimental setup. Specifically, we are working to reduce the crosstalk from the loudspeaker to the detector. This crosstalk is caused by the strong magnetic field from the magnet in the loudspeaker. The vibration on the detector causes it to cut the magnetic flux lines from the speaker, generating a current. To reduce the crosstalk, we twisted the wires connecting the detector in order to reduce the effective magnetic flux enclosed by the wires. Electric shielding has also been applied. We are also working on the alignment of the detector to ensure that the direction of the vibration lies on the optical axis.